Vietnam Journal of Mathematics **38**:3(2010) 323-339

Vietnam Journal
of
MATHEMATICS

Numerical Simulation of a Single-Mode Richtmyer-Meshkov Instability Using Conservative Front Tracking Method

M. A. Ullah, Gao Wenbin, and Mao De-kang

Department of Mathematics, Shanghai University,
Shanghai 200444, P. R. China

Received April 30, 2010

Abstract. The conservative front-tracking method developed in [15, 16], with the 5^{th}-order WENO scheme developed in [11] as the underlying scheme, uses 1D hyperbolic conservation laws to describe the motion of the interface and discretizes them by the Lax-Wendroff (LxW) scheme in some way. In this paper, we use this method to simulate a single-mode Richtmyer-Meshkov instability (RMI). The purpose is to test the ability of this front-tracking method to simulate the RMI, especially its advantages over capturing schemes. On a coarse grid the simulation gives a much better result than the capturing simulation. The interface with roll-ups is well resolved, the discontinuity in density is sharply represented without width, and the smooth solution on the two sides of the interface is well computed. This is because the method includes no numerical dissipation across the tracked interface, and the numerical dispersion of the LxW scheme for tracking the interface serves as a numerical surface tension, which regularizes the interface in the simulation. However, in the simulation on a finer grid, though the main structure of the interface is well resolved, the discontinuity in density is sharply represented and the smooth solution on the two sides of the interface is well computed, the roll-ups of the interface develop complex, maybe incorrect, structures, which finally terminates the simulation at an intermediate time. The reason is that the LxW scheme for tracking the interface is not yet good enough for regularizing the interface. In our future development of the method the LxW scheme will be replaced with better schemes, such as the TVD schemes that include numerical dissipation.

2000 Mathematics Subject Classification: 65M06, 35Q53.

Key words: Richtmyer-Meshkov instability, conservative front-tracking, Lax-Wendroff scheme, numerical surface tension.

1. Introduction

The Richtmyer-Meshkov instability (RMI) is a shock-induced instability phenomena in fluid dynamics. When an incident shock collides with a perturbed contact discontinuity between two fluids of different densities, the contact discontinuity becomes unstable and small perturbations of this interface grow into nonlinear structures having the form of "bubbles" and "spikes". The flow may involve different fluids, and in this case, the contact discontinuity is actually a material interface. The RMI has practical applications in many fields, such as Inertial Confinement Fusion (ICF), supernova explosion and supersonic combustion.

When the fluid is compressible, the evolution of fluid motion is governed by the Euler system, see (7)-(11), to which the exact solutions are difficult to obtain, especially those of the RMI. Laboratory experiments investigating the RMI are usually expensive and not quite accurate; the effects of the thin membrane that separate the two fluids and/or the mass diffusion across the interface impede obtaining a highly quantitative observation of the phenomena, see [1, 3, 20] and the references cited therein. Therefore, the numerical simulations began to play important roles and are expected to give qualitative and quantitative understanding of the RMI.

A standard view of the numerical simulation of the RMI is that the numerical solutions should be convergent and stable, hopefully in the sense that under mesh refinement the large scale structures of the solutions converge and the small scale structures that emerge with the mesh refinement will be controlled, at least they do not influence the large scale ones. However, this standard view is often failed to be met in the numerical simulations of the RMI using capturing methods. Numerical solutions often do not converge under mesh refinement, and if they do, different codes can converge to different solutions. This kind of situations occur in simulations to or after the intermediate times when roll-ups have developed, see [12, 13, 21, 23] and the references cited therein. Simulations with lower order schemes on coarse grids are usually poor in the resolutions of the roll-ups and the smooth solution on the two sides of the interface. Refining the grids and using high order schemes help little to enhance the resolution but trigger numerical secondary structures near the interface, which pollute the simulations.

As Glimm pointed out in [4], the real flow includes small scale physics of dissipation, mass diffusion, viscosity and heat conduction, and in this sense the real flow is actually governed by a parabolic system, the Navier-Stokes equations. This physics of dissipation is a necessary regularization, without which the flow will not be stable. However, in the numerical simulations, the numerical dissipations of the capturing methods supplement the missing regularization from the physics, especially across the interface, and in this way the numerical secondary structures emerge under mesh refinement and eventually pollute the large scale structures.

The front-tracking methods treat discontinuities, shocks and/or interfaces, in the flow as interior moving boundaries. Solutions on the two sides of the discontinuities are computed using schemes stable and convergent for smooth solutions, and the discontinuities are tracked with their moving velocities. The main advantage of the front-tracking methods is that they eliminate the numerical dissipation across the interface that is inherent in the capturing methods. The front-tracking method developed by Glimm and his co-workers, see [2, 5, 6, 7] and the references cited therein, is proved to be efficient in the RMI simulations. Their front-tracking simulations of RMI in [8, 9, 10] produced significantly better agreement with the experimentally measured growth rates than obtained in non-tracking computations. However, Glimm's front-tracking method is complex in algorithm and coding, and maintaining the conservation in the method is not an easy job, see the above cited references.

In recent years, Mao developed a front-tracking method for the 2D Euler system, see [15, 16], and the early work can be traced back to 90's of the last century, see [17, 18, 19]. Like all the front-tracking methods, it includes no numerical dissipation across the tracked interface. However, the following two features distinguish it from the other front tracking methods: 1) The discontinuity curves are tracked by enforcing the conservation properties of the Euler system rather than by the moving velocity of the discontinuities. 2) The motion of discontinuity curves is locally described by 1D hyperbolic conservation laws (HCL's) derived from the Euler system, and the tracking is performed by locally discretizing these 1D HCL's on Cartesian sub-grids. In the current algorithm these 1D HCL's are discretized by the Lax-Wendroff (LxW) scheme in some way. Also the 5^{th}-order WENO scheme developed in [11] is adopted as the underlying scheme of the tracking method. Designed in such a way, Mao's front-tracking method is much simpler than the other front-tracking methods, it runs on Cartesian grids and uses no adaptive grids, and more important, it is fully conservative.

In this paper, we use Mao's front-tracking method to simulate a single-mode RMI flow. The purpose is to test the ability of this method to simulate the RMI, especially the ability to resolve the roll-up structures to and after the intermediate times. As is described in the above, the method does not include numerical dissipation across the tracked interface. Also the numerical dispersion included in the LxW scheme that discretizing the 1D HCL's will serve as a numerical surface tension to regularize the tracked interface, see the discussion in Subsec. 2.3. In this way, the method is expected to give much better results than capturing simulations even on coarse grids.

The numerical simulation verifies this expectation. In the simulation on a coarse grid, the interface with roll-ups is well resolved, the discontinuity in density is sharply represented without width, the smooth solution in the bubbles and spikes are well computed, and the velocity and pressure, which are continuous across the interface, are comparable to that of capturing simulation. In the simulation on a finer grid, the main structure of the interface is still well resolved, the discontinuity in density is still sharply represented without width, and the smooth solution in the bubbles and spikes are still well computed. Compared with

the result on the coarse grid, the main structure of the interface and the velocity and pressure show good convergence. However, the roll-ups of the interface occur earlier than on the coarse grid and develop complex, maybe incorrect, structures that finally terminates the simulation. Nevertheless, the complex structures are not of the numerical secondary type as reported in [12, 13, 21, 23]. The numerical simulation indicates that the LxW scheme discretizing the 1D HCL's is not yet good enough for regularizing the interface, see the discussion in Subsec.3.2. Currently, we are considering to replace it with the TVD type schemes, which include numerical dissipation rather than dispersion, see [14], to improve the method.

The paper is organized in the following way: Sec. 1 is the introduction. In Sec. 2, we briefly describe Mao's conservative front-tracking method. In Sec. 3, we describe the single-mode RMI problem to be simulated and report our numerical results. Finally, Sec. 4 is the conclusion.

2. Conservative Front-Tracking Method

In this section, we are going to give a brief description of the conservative front-tracking method developed in [15, 16], focusing mainly on the ideas and the strategies. The details of the method can be found in the cited references.

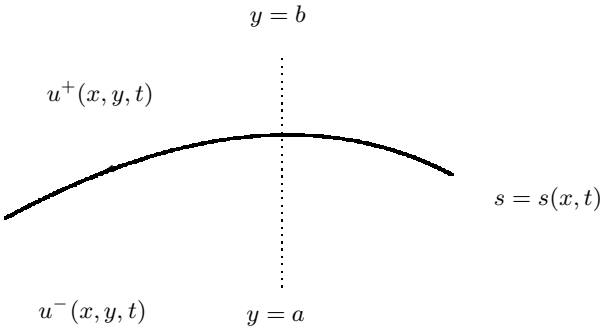

Fig. 1 The solution is piecewise smooth and involves one discontinuity curve, which is defined by a function $y = s(x, t)$ at time t.

We consider a 2D hyperbolic conservation law

$$u_t + f(u)_x + g(u)_y = 0, \tag{1}$$

where u, $f(u)$ and $g(u)$ can be either scalars or vectors. We assume that the solution involves only one discontinuity curve as shown in Fig. 1, on the two sides of which the solution, denoted by $u^-(x, y, t)$ and $u^+(x, y, t)$, respectively, is smooth. An orientation is defined on the curve so that u^- is on the left and u^+ is on the right. We start our description with the scalar case in Subsec. 2.1,

Subsec. 2.2 and Subsec. 2.3, where u, $f(u)$ and $g(u)$ are all scalars, and then extend the method to the Euler system in Subsec. 2.4. In Subsec. 2.1 we find the 1D HCL's that locally describe the motion of the discontinuity curve, in Subsec. 2.2. we describe the data structure of the numerical solution, and in Subsec. 2.3 we describe the algorithm of our conservative front-tracking method.

2.1. 1D HCL's That Locally Describe the Motion of Discontinuity Curve

Firstly, we assume that the discontinuity curve can be locally defined as a smooth function $y = s(x,t)$ at time t as shown in Fig. 1, and we say that the curve is locally of y-type. We integrate (1) with respect to y from $y = a$ to $y = b$, with a and b two constants, and obtain

$$\frac{\partial \int_a^b u(x,y,t)dy}{\partial t} + \frac{\partial \int_a^b f(u(x,y,t))dy}{\partial x} + g(u^+(x,b,t)) - g(u^-(x,a,t)) = 0. \quad (2)$$

We denote by $U_{(a,b)}(s(x,t))$ and $F_{(a,b)}(s(x,t))$ the two integrals in (2),

$$U_{(a,b)}(s(x,t)) = \int_a^b u(x,y,t)dy = \int_a^{s(x,t)} u^-(x,y,t)dy + \int_{s(x,t)}^b u^+(x,y,t)dy$$

and

$$F_{(a,b)}(s(x,t)) = \int_a^b f(u(x,y,t))dy = \int_a^{s(x,t)} f(u^-(x,y,t))dy + \int_{s(x,t)}^b f(u^+(x,y,t))dy,$$

and view $s(x,t)$ as an unknown and $u^{\pm}(x,y,t)$ as known. With these notations, equation (2) reads

$$\frac{\partial U_{(a,b)}(s(x,t))}{\partial t} + \frac{\partial F_{(a,b)}(s(x,t))}{\partial x} + G_{(a,b)}(x,t) = 0, \quad (3)$$

with $G_{(a,b)}(x,t) = g(u^+(x,b,t)) - g(u^-(x,a,t))$ a known function. Secondly, we assume that the discontinuity curve can be locally defined as a smooth function $x = w(y,t)$ at time t, and we say that the curve is locally of x-type. By the same arguments, a PDE similar to (3) on the x-direction is also obtained

$$\frac{\partial V_{(c,d)}(w(y,t))}{\partial t} + \frac{\partial G_{(c,d)}(w(y,t),y,t)}{\partial x} + F_{(c,d)}(y,t) = 0, \quad (4)$$

with $F_{(c,d)}(y,t) = f(u^+(d,y,t)) - f(u^-(c,y,t))$ a known function.

We should note that for a smooth discontinuity curve, its local motion can always be described by either (3) or (4). These equations are the basis of our

conservative front-tracking method. We note that (3) and (4) are both 1D conservation laws, only that the unknowns $s(x,t)$ and $w(y,t)$ appear in nonlinear functions U and V. It is shown in [15] that (3) and (4) are both hyperbolic and equivalent to the Hugoniot condition across the discontinuity curve.

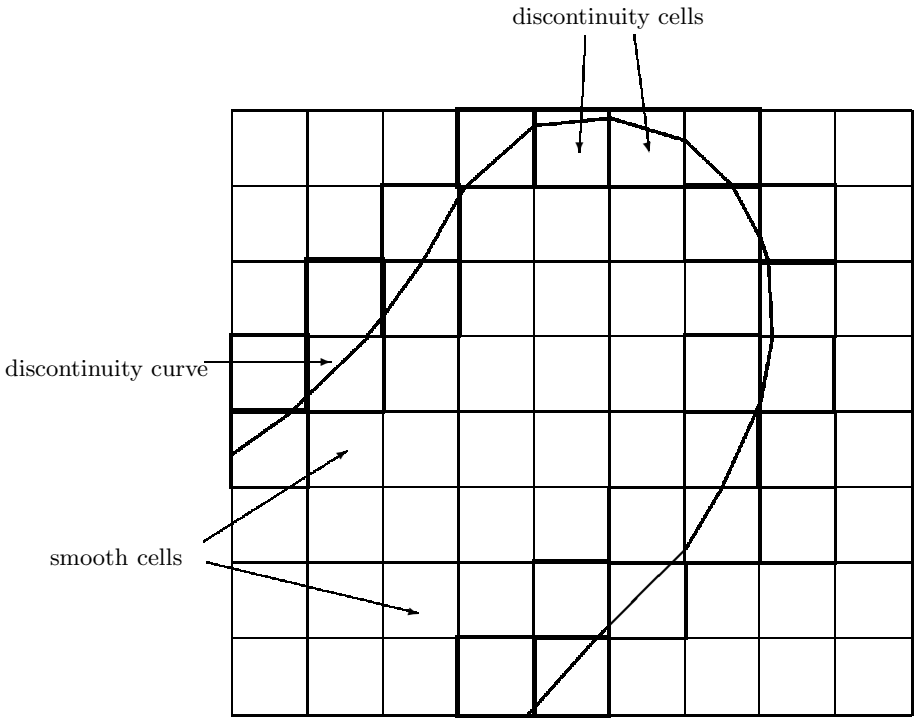

Fig. 2 Smooth cells and discontinuity cells two space dimensions

2.2. Numerical Solution

The numerical solution, defined on a fixed Cartesian grid, is a cell-average approximation to the true solution,

$$u_{i,j}^n \simeq \frac{1}{h^2} \int_{x_{i-1/2}}^{x_{i+1/2}} \int_{y_{j-1/2}}^{y_{j+1/2}} u(x,y,t_n)dydx. \tag{5}$$

A discontinuity curve is represented by a list of cells that are crossed by the curve as shown in Fig. 2. We call these cells the discontinuity cells, and call the cells in smooth region the smooth cells. The numerical solution in each discontinuity cell has three cell-average approximations, the left cell-average $u_{i,j}^{n,-}$, which approximates $u^-(x,y,t)$, the right cell-average $u_{i,j}^{n,+}$, which approximates $u^+(x,y,t)$, and the ordinary cell-average $u_{i,j}^n$, which is the cell-average approximation in the sense of (5). Once all the cell-averages are computed, the disconti-

nuity curve can be recovered from them by enforcing the conservation property of the solution.

2.3. Algorithm

A finite volume scheme,

$$u_{i,j}^{n+1} = u_{i,j}^{n} - \lambda \left(\hat{f}_{i+\frac{1}{2},j}^{n} - \hat{f}_{i-\frac{1}{2},j}^{n} \right) - \lambda \left(\hat{g}_{i,j+\frac{1}{2}}^{n} - \hat{g}_{i,j-\frac{1}{2}}^{n} \right), \tag{6}$$

is adopted as the underlying scheme. In our front-tracking algorithm, the 5^{th}-order WENO scheme developed in [11] is used as the underlying scheme. The numerical solution in smooth region, which includes cell-averages in all the smooth cells and $u_{i,j}^{n,\pm}$'s in all the discontinuity cells, is computed with the underlying scheme (6). Whenever the stencil of the scheme is across the tracked discontinuity curve and data on the other side of the curve are requested in the computation, which happens in the cells near the discontinuity curve and in computing the left and right states $u_{i,j}^{n,\pm}$ in discontinuity cells, extrapolation data from the side in computation are used. In this way, the computation on each side of the discontinuity curve uses information only from the same side. Once the cell-averages in all smooth cells and the left and right cell-averages in all discontinuity cells are computed, the solution on each side of the discontinuity curve, i.e. $u^{\pm}(x, y, t_{n+1})$, can be reconstructed point-wisely up to the curve.

To track the discontinuity curve, we discretize equations (3) and (4) in the vicinity of every discontinuity cell, on either x- or y-subgrid, to compute the ordinary cell-average in the cell, using the reconstructed $u^{\pm}(x, y, t_{n+1})$ and the numerical fluxes in computing the solution in the smooth region. Since (3) and (4) are both 1D HCL's, there are well-developed numerical methods for discretizing them. In our algorithm, we use the LxW scheme to discretize the equations in some way. Once the ordinary cell-averages in the discontinuity cells are computed, the segments of the discontinuity curve in the cells are then recovered. Thus, we complete a step of computation.

The LxW scheme includes numerical dispersion, see [14], which assures the linear stability of the scheme. When discretizing (3) and (4), this numerical dispersion is not of 2D that stabilizes the numerical solution on the two sides of the discontinuity curve, but of 1D that regularizes the discontinuity curve. It serves as a numerical surface tension on the discontinuity curve to control the emergence of small scale structures. This is one of the merits of our front-tracking method.

2.4. Extension to the Euler System

The 2D Euler system of gas dynamics is

$$\frac{\partial \phi}{\partial t} + \frac{\partial F(\phi)}{\partial x} + \frac{\partial G(\phi)}{\partial y} = 0, \tag{7}$$

$$\phi = (\rho, u\rho, v\rho, \rho e)^T, \tag{8}$$

$$F(\phi) = (\rho u, \rho u^2 + p, \rho uv, (\rho e + p)u)^T, \tag{9}$$

$$G(\phi) = (\rho v, \rho uv, \rho v^2 + p, (\rho e + p)v)^T, \tag{10}$$

$$p = (\gamma - 1)\left(\rho e - \frac{1}{2}\rho(u^2 + v^2)\right), \tag{11}$$

where ρ, u, v, p, and e are the density, x-component and y-component of velocity, pressure, and total energy, respectively, and γ is the ratio of specific heats.

The method can be straightforwardly extended to the Euler system, only we need to note that ϕ, $F(\phi)$ and $G(\phi)$ are now vectors with four components. Numerical solution in smooth region is computed with the 5^{th}-order WENO scheme developed in [11] and the 1D HCL's are discretized with LxW scheme, which includes numerical dispersion. The Euler system has three different characteristic fields and thus three different kinds of discontinuities. When tracking a discontinuity of a certain kind, waves in other characteristic fields may propagate across it. In the tracking method for the Euler system, 1D Riemann problems are solved at the discontinuity curve in the normal directions, and based on which waves related to the other characteristic fields are separated from the cell-averages in the discontinuity cell and are then transported to the corresponding sides. Also, (3) and (4) are both systems of four equations, and the numerical solutions of them will provide us locally with four recovered segments of the discontinuity curve. A weighted result is adopted as the final result for the curve. However, when tracking an interface, we take the segment recovered from the density as the final result, considering that the interface is essentially a discontinuity of mass, across which the velocity and pressure are continuous.

3. Numerical Simulation of a Single-Mode RMI

3.1. The Single-Mode RMI

A shock strikes an interface separating polytropic gases ($\gamma = 1.4$) of different densities, and the initial setup is as shown in Fig 3. The solution region is $(0, 1)\times(-1, 1)$. The downward-going shock of Mach number 5.0 is initially located at $y = 0.4$. The interface is sinusoidally perturbed with wavelength 1.0 and amplitude 0.1, and located at $y = 0$. The density ratio across the interface is 5.0. Flow-through boundary conditions are on the top and bottom and periodic boundary conditions are on the two sides. To keep the interface staying in the region in the simulation, an upward translation velocity of 3.128 is added. In the simulation, the interface is tracked, but the shock is captured by the underlying WENO scheme.

This problem is suggested in [5] and used by the authors of that paper to test their conservative and nonconservative front-tracking methods. We choose this problem because the solution region is not large and the roll-up structures occur early because of the rather strong shock and perturbation of the interface. The simulation is thus of intermediate size in both memory and CPU compared with

that in [8, 9, 12, 13, 21]; however, there is no experimental result for comparison. Currently we do not have the computer resource for long-time simulation in large region.

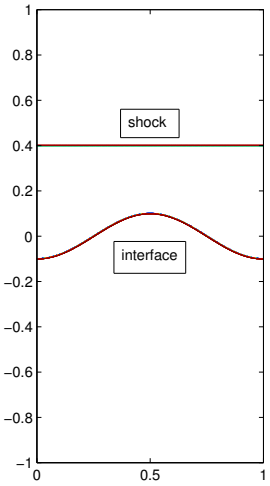

Fig. 3 The setup of the single-mode RMI, a downward-going shock with Mach number 5.0 strikes a sinusoidally perturbed interface

3.2. Numerical Results

We first conduct the numerical simulation on a grid of 81×161 cells, and the numerical results at times $t = 1.38$ and 2.4 are displayed in Fig. 4 and Fig. 5. The first is the simulation time in [5] and the second is a late-intermediate time for the RMI. In each figure we present the tracked interface in the upper-half region, the 3D image of the density in an upper-left subregion, and the contours of the x-velocity and pressure in the upper-half region. As is described in the previous section, the solution on each side of the interface is computed independently using information only from the same side, and thus it can be reconstructed point-wisely on each side, using the left and right cell-averages, up to the tracked interface. We thus project the reconstructed solution onto a finer grid and then use the Matlab to draw the 3D images of the density. We present the 3D images of the density in order to show that the discontinuity in density is sharply represented without width in our simulation. In Fig. 6 we present the numerical amplitude and growth rate of the single-mode RMI up to the time 2.4.

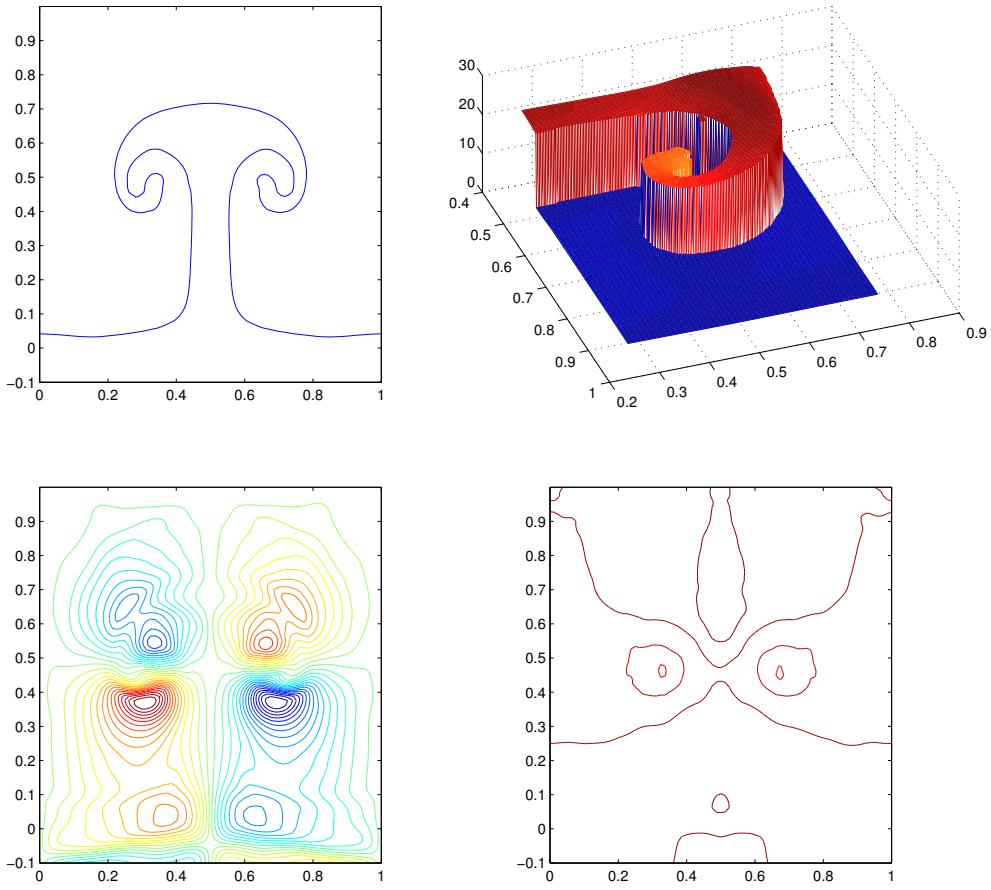

Fig. 4 Numerical solution obtained by the conservative front-tracking on a 81×161 grid at $t = 1.38$, from the left to the right and from the top to the bottom are the tracked interface, the 3D image of the density, and the contours of the x-velocity and pressure.

For comparison, we also present the numerical solutions computed by the underlying WENO scheme, without tracking, on a grid of 161×320 cells at the same times in Fig. 7 and Fig. 8, respectively. In each figure we present the contour of the density in the upper-half region, the 3D image of the density in the same upper-left subregion, and the contours of the x-velocity and pressure in the upper-half region.

Comparing the tracking and WENO results we have the following observations:

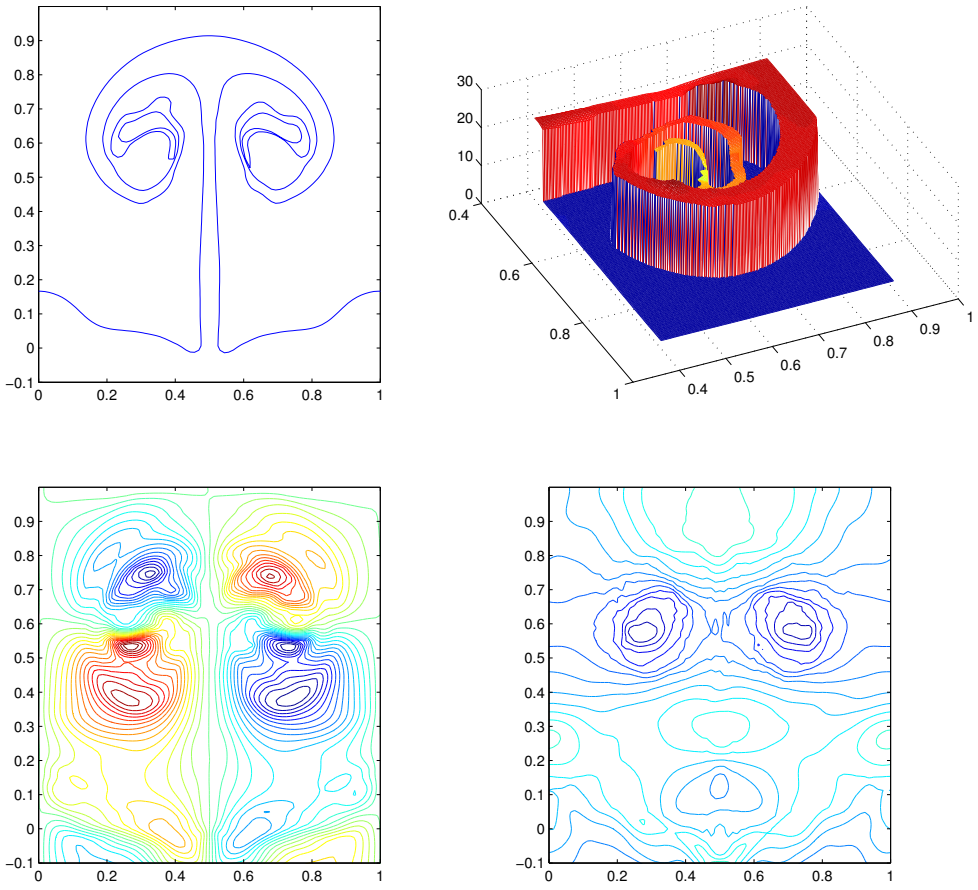

Fig. 5 Numerical solution obtained by the conservative front-tracking on a 81×161 grid at $t = 2.4$, from the left to the right and from the top to the bottom are the tracked interface, the 3D image of the density, and the contours of the x-velocity and pressure.

1) The tracking solution includes no numerical diffusion in the density, the discontinuity in density is sharply presented without width, and the smooth solution in both the bubbles and spikes is well computed, which can be clearly seen in the 3D images of the density. On the other hand, the discontinuity in density in the WENO solution is severely diffused, especially the roll-ups, even the solution is obtained on a finer grid. We should point out that the numerical diffusion in the WENO solution can not be reduced simply by refining the grid and/or using higher order schemes, which may help little to sharpen the discontinuity but to trigger the nonphysical secondary structures as reported in [15, 12, 13, 21].

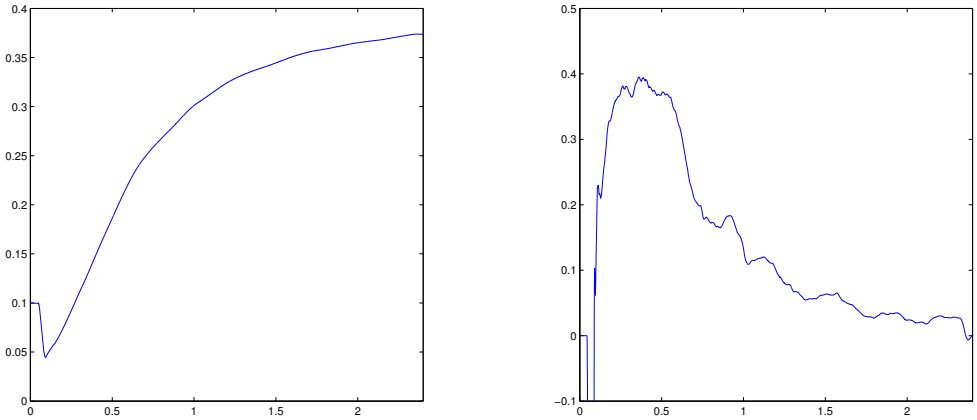

Fig. 6 The amplitude(left) and growth rate(right) of the single-mode RMI.

2) The tracked interface with roll-ups is well resolved even to the late-intermediate time, and it is kept smooth in the whole simulation without secondary structures emerged. This should thank to the numerical surface tension provided by the LxW scheme as described in the previous section, which keeps regularizing the interface in the simulation. However, the roll-ups in the tracking solution occur a bit later compared with the WENO solution, which is also because of the numerical surface tension.

3) The x-velocity and pressure of the tracking and WENO solutions are comparable with each other, only the x-velocity and pressure of the WENO solution have higher resolution because they are computed on a finer grid.

Next we conduct the numerical simulation on a grid of 161×321 cells and the numerical result at $t = 1.38$, the tracked interface, 3D image of the density, and contours of the x-velocity and pressure, is presented in Fig. 9. It is seen from the figure that the main structure of the tracked interface is still well resolved and shows good convergence compared with that on the coarse grid. The discontinuity in density is still sharply presented with the solution well resolved in both the the bubbles and spikes. Also the x-velocity and pressure show good convergence compared with that on the coarse grid. However, the roll-ups of the spikes occur earlier and grow faster than that on the coarse grid and develop complex structures. The roll-ups on the left and right are not symmetric, and the structure of the left one does not look right. Nevertheless, the tracked interface is still kept smooth in some sense and there is no secondary structures near it.

The simulation is terminated at around $t = 1.419$ because of the complex, maybe incorrect, structure of the left roll-up, which the current code can not handle.

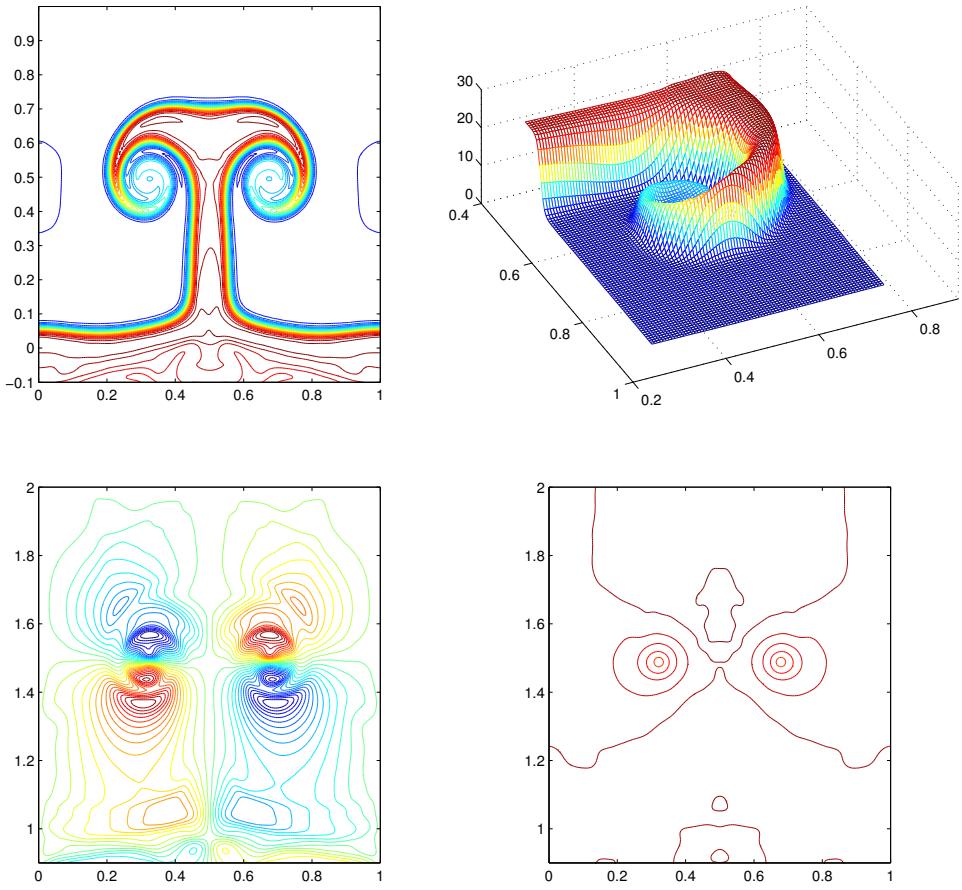

Fig. 7 Numerical solution obtained by the 5th-order WENO scheme on a 161×321 grid at $t = 1.38$, from the left to the right and from the top to the bottom are the contour of density, the 3D image of the density, and the contours of the x-velocity and pressure.

We find that the development of complex, maybe incorrect, structures of the interface, which finally terminates the simulation, is due to that the LxW scheme that discretizing the 1D HCL's (3) and (4) is still not good enough for regularizing the tracked interface. We find that the problems happen when corners of the interface are generated, where the interface is not smooth and where the LxW scheme is not able to smoothen the corners, see [15]. Some corners develop into complex, maybe incorrect, structures in the following computation and thus ruin the simulation. Currently, we are considering to use schemes with TVD properties to discretize the equations (3) and (4). The schemes with TVD properties include numerical dissipation rather than dispersion, see [14], which we believe

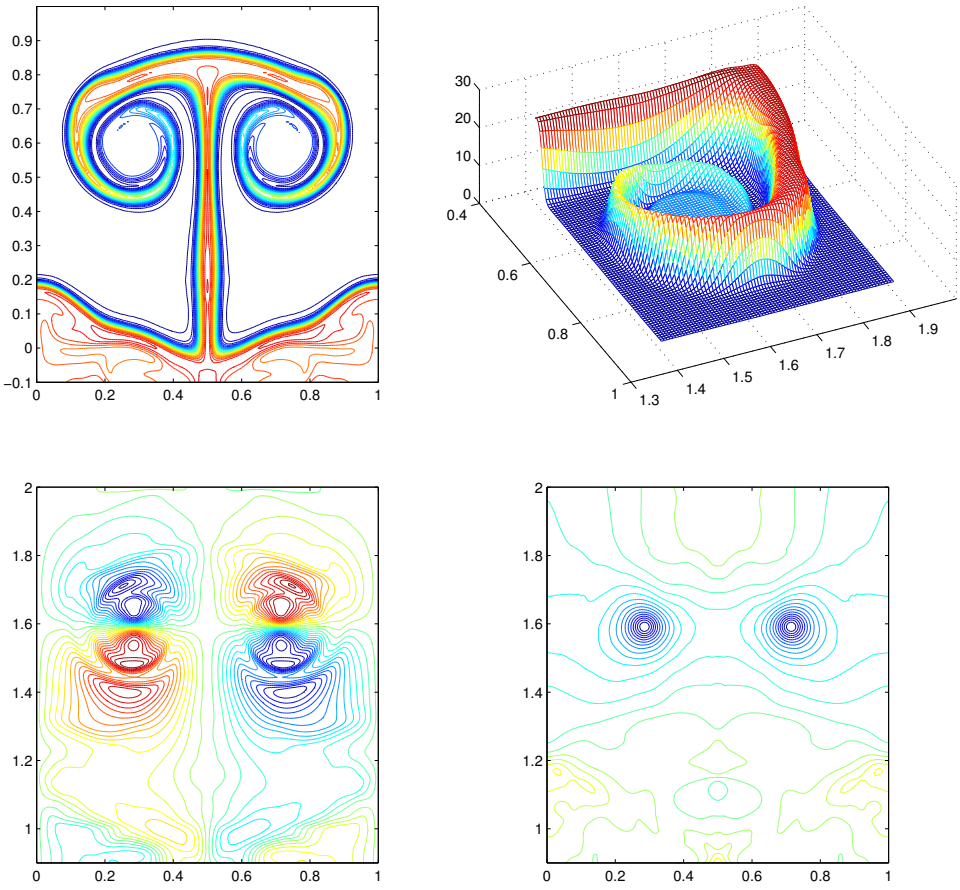

Fig. 8 Numerical solution obtained by the 5th-order WENO scheme on a 161×321 grid at $t = 2.4$, from the left to the right and from the top to the bottom are the contour of density, the 3D image of the density, and the contours of the x-velocity and pressure.

may be able to control the development of complex structures. The modification is underway and it is expected that in our future numerical simulations of the RMI the development of complex structures can be controlled while the main structure of the interface and the velocity and pressure will still be convergent under mesh refinement.

Finally, we note that the numerical simulation of the same RMI presented in [5] with Glimm's front-tracking method does not well resolve the roll-up structures, even on a grid of 160×320 cells. At this point we believe that our numerical simulation is better than theirs. We think this should thank to the conservation feature of our front-tracking method. In our method, the conservation of the

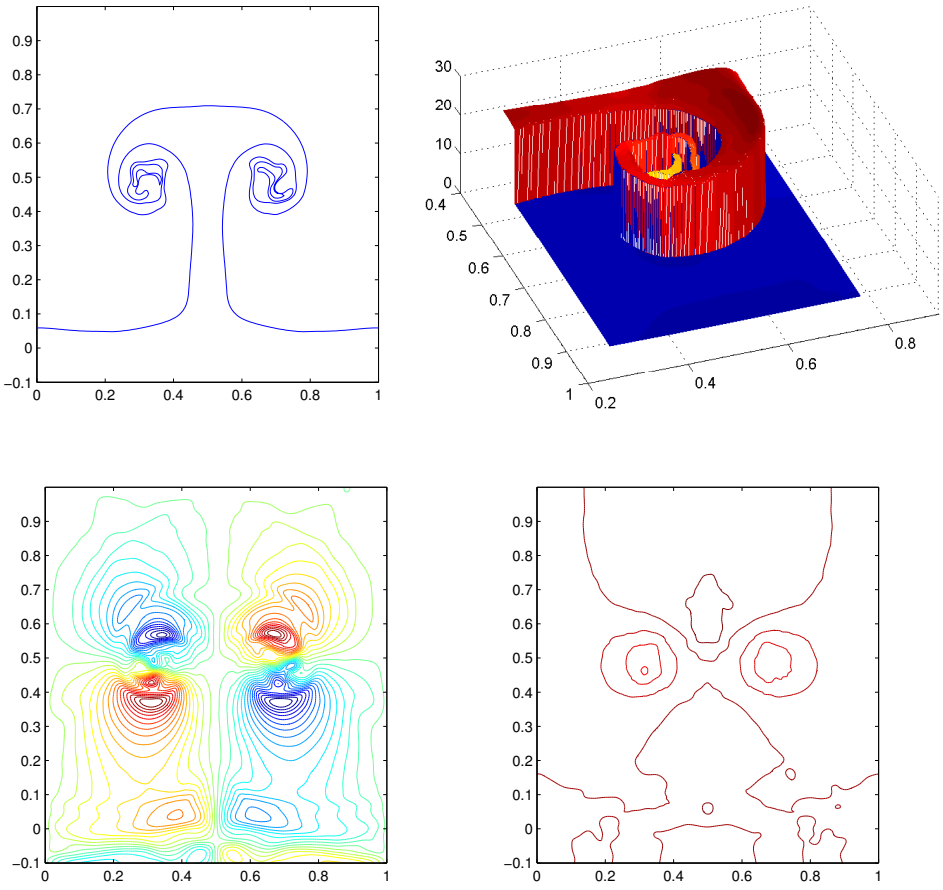

Fig. 9 Numerical solution obtained by the conservative front-tracking on a 161×321 grid at $t = 1.38$, from the left to the right and from the top to the bottom are the tracked interface, the 3D image of the density, and the contours of the x-velocity and pressure.

solution is the tracking mechanism rather than merely properties to be maintained.

4. Conclusion

We have used Mao's conservative front-tracking method to simulate a single-mode RMI. The simulation on a coarse grid gives a much better result than the capturing simulation using the underlying WENO scheme. The solution in smooth region, especially in the bubbles and spikes, is well computed, and the

interface with roll-ups is sharply represented without width. In the simulation on a finer grid, the solution in smooth region is still well computed and shows convergence, and the interface is still sharply represented without width. However, the roll-ups occur earlier and develop complex, maybe incorrect, structures, which finally terminates the simulation at an intermediate time. We believe that the LxW scheme that discretizes the 1D HCL's for tracking is not good enough for regularizing the tracked interface and should be replaced by schemes with TVD properties in the future development of the method.

Acknowledgments. The authors wish to thank the referees for their valuable comments and suggestions, which really helped us in revising the paper. This work was supported by the Shanghai Pu Jiang Program [2006] 118.

References

1. R. Aure and J. W. Jabocs, Particle image velocimetry study of shock-induced single mode Richtmyer-Meshkov instability, *Shock Waves* **18** (2008), 161–167.
2. I.-L. Chern, J. Glimm, O. McBryan, B. Plohr, and S. Yaniv, Front tracking for gas dynamics, *J. Comput. Phys.* **62** (1986), 83–110.
3. B. D. Collins and J. W. Jacobs, PLIF flow visualization and measurements of the Richtmyer-Meshkov instability of an air/SF_6 interface, *J. Fluid Mech.* **464** (2002), 113–136.
4. J. Glimm, *The Mathematics and Numerics of Chaotic Mixing Flows,* Talk in the Joint Meeting of the American Mathematical Society and Shanghai Mathematical Society, Fudan Univ. Shanghai, 2008.
5. J. Glimm, X. L. Li, Y. J. Liu, Z. L. Xu, and N. Zhao, Conservative front-tracking with improve accuracy, *SIAM. J. Numer. Anal.* **41** (5) (2003), 1926–1947.
6. J. Glimm, M. J. Graham, J. Grove, X. L. Li, T. M. Smith, D. Tan, F. Tangerman, and Q. Zhang, Front tracking in two and three dimensions, *Comput. Math. Appl.* **35** (1998), 1–11.
7. J. W. Grove, R. Holmes, D. H. Sharp, Y. Yang and Q. Zhang, Quantitative theory of Richtmyer-Meshkov instability, *Phys. Rev. Lett.* **71** (1993), 3473–3476
8. R. L. Holmes, *A numerical Investigation of the Richtmyer-Meshkov Instability Using Front-Tracking*, Doctor's dissertation, State University of New York at Stony Broke, 1994.
9. R. L. Holmes, J. W. Grove, and D. H. Sharp, A numerical investigation of the Richtmyer-Meshkov instability using front-tracking, *J. Fluid Mech.* **301** (1995), 51–64.
10. R. L. Holmes et al., Richtmyer-Meshkov instability growth: experiment, simulation and theory, *J. Fluid Mech.* **389** (1999), 55–79.
11. G.-S. Jiang and Chi-Wang Shu, Efficient Implementation of Weighted ENO Schemes, *J. Comput. Phys.* **126** (1996), 202–228.
12. M. Latini, O. Schilling, and W. S. Don, Effects of WENO flux reconstruction order and spatial resolution on reshocked two-dimensional Richtmyer-Meshkov instability, *J. Comput. Phys.* **221** (2007), 805–836.
13. M. Latini, O. Schilling, and W. S. Don, High-resolution simulation and modelling of reshocked single-mode Richtmyer-Meshkov instability: Comparison to experimental data and to amplitude growth model preditions, *Phys. Fluids* **19** (2007), 024104.
14. R. J. LeVeque, *Finite Volume Methods for Hyperbolic Problems,* Published by the press Syndicate of the University of Cambridge, 2002.

15. D. K. Mao, Towards front-tracking based on conservation in two space dimensions II, tracking discontinuities in capturing fashion, *J. Comput. Phys.* **226** (2007), 1550–1588.
16. D. K. Mao, Towards front tracking based on conservation in two space dimensions, *SIAM. J. Sci. Comput.* **22** (1) (2000), 113–151.
17. D. Mao, A shock tracking technique based on conservation in one space dimmension, *SIAM J. Numer. Anal.* **32** (1995), 1677–1703.
18. D. Mao, A treatment of discontinuities for finite difference method in the two dimensional case, *J. Comput. Phys.* **104** (1993), 377–397.
19. D. Mao, A treatment of discontinuities for finite difference methods, *J. Comput. Phys.* **103** (1992), 359–369.
20. E. E. Meshkov, Instability of a shock wave accelerated interface between two gases, *NASA Tech. Trans.* **F-13** (1970), 074.
21. G. Peng, N. J. Zabusky, and S. Zhang, Vortex-accelerated secondary baroclinic vorticity deposition and late-intermediate time dynamics of a two-dimensional Richtmyer-Meshkov interface, *Phys. Fluids* **15** (2003), 3730–3744.
22. R. D. Richtmyer, Taylor instability in shock acceleration of compressible fluids, *Commun. Pure Appl. Math.* **13** (1960), 297–319.
23. J. Shi, Y. Zhang, and C. W. Shu, Resolution of high order WENO schemes for complicated flow structures, *J. Comput. Phys.* **186** (2003), 690–696.